Techno-Economic Assessment of Sour Gas Oxy-Combustion Water Cycles for CO_2 Capture

N.W. Chakroun*, A.F. Ghoniem

Massachusetts Institute of Technology, Department of Mechanical Engineering
77 Massachusetts Ave., Cambridge, MA 02139, United States

Abstract

Growing energy demand coupled with the threat of global warming call for investigating alternative and unconventional energy sources while reducing CO_2 emissions. One of these unconventional fuels is sour gas, which consists of methane, hydrogen sulfide and carbon dioxide. Using this fuel poses many challenges because of the toxic and corrosive nature of its combustion products. A promising technology for utilizing it is oxy-fuel combustion with carbon capture and storage, including the potential of enhanced oil recovery for added economic benefits. Although methane oxy-fuel cycles have been studied in the literature, using sour gas as the fuel has not been investigated or considered. In this paper, water is used as the diluent to control the flame temperature in the combustion process, and the associated cycle type is modeled to examine its performance. As the working fluid condenses, sulfuric acid forms which causes corrosion. Therefore, either expensive acid resistant materials should be used, or a redesign of the cycle is required. These different options are explored. A cost analysis of the proposed systems is also conducted to provide preliminary estimates for the levelized cost of electricity (LCOE). The results show the acid resistance cycle with a 4.5% points increase in net efficiency over the cycle with SO_x removal. However there is nearly a 9% decrease in the cycle's LCOE for the latter case.

Keywords: Oxy-fuel combustion, Power cycle analysis, CO_2 capture and sequestration, Sour gas

1. Introduction

Greenhouse gas (GHG) emissions are the leading contributers to climate change. Combustion of fossil fuels results in the formation of significant amounts of carbon dioxide (CO_2), the primary GHG released into the atmosphere. At the global scale, CO_2 emissions accounted for approximately 77% of all GHG emissions in 2007 [1]. According to the Environmental Protection Agency (EPA), about 26% of all global GHG emissions were produced by the electricity generation sector. It is also estimated that the world CO_2 emissions from electricity production will increase by approximately 43% by 2035, from 30.2 billion metric tons in 2008 to

*Corresponding author
Email address: nwc@mit.edu, Telephone number: +1 (765) 409-7402

43.2 billion metric tons in 2035 [2]. Much of this growth in emissions is attributed to the developing non-OECD countries which continue to rely on fossil fuels to meet their growing energy demand. By 2040, these non-OECD countries are expected to contribute as much as 69% of the world's total emissions, whereas the OECD emissions, totaling about 14 billion metric tons, represent the balance [2]. Emissions reductions are vital for the world and the developing nations with their ever increasing populations and energy demands.

The International Energy Agency (IEA) has identified carbon capture and storage (CCS) as one of the important strategies in reducing CO_2 emissions [3]. In this technology, CO_2 released from power plants is separated, compressed and transported to a site for underground injection in secure geological formations, including natural underground reservoirs, or depleted oil and gas fields. The integration of these CCS technologies with the power generation plants has not yet been fully demonstrated commercially at a large enough scale that can overcome the technological risk and cost barriers [4, 5]. Nonetheless, oxy-fuel combustion is one of the promising CCS options [6], the other ones being post-combustion CO_2 capture and pre-combustion CO_2 capture [7]. The main difference between these technologies is the location at which the CO_2 is removed in the cycle. In oxy-fuel combustion, the fuel is burned in oxygen diluted with CO_2 or water, at near stoichiometric conditions so that the products consist of only carbon dioxide and water. The water can then be easily separated from the carbon dioxide by condensation. A diluent is added to the fuel and oxidizer to moderate the temperatures in the combustion chamber. Due to the simplicity of the carbon capture system in oxy-fuel combustion, the CO_2 capture efficiency is very high (90% +) [7]. This is one of the main reasons for the recent interest in this CCS technology.

Oxy-combustion has often been associated with coal since coal power plants produce about two times as much CO_2 per MWh than natural gas power plants [1]. On the other hand, natural gas' share of the world's electricity generation is expected to grow from 22% in 2010 to 24% in 2040 [2] and applying the same concept to this fuel has been suggested. Estimated cost of electricities by source [8], suggest that natural gas cycles for CCS are competitive with other zero carbon energy sources. For our analysis we will be focusing on an even cheaper source of natural gas, namely sour gas.

Sour gas consists of three major components: methane (CH_4), hydrogen sulfide (H_2S) and CO_2. This is the form of natural gas extracted, from a growing number of gas fields, prior to the purification process [9]. Typical volume fractions of the H_2S and CO_2 compounds are between 0-30% each, the exact composition changes depending on the life of the well, location and geography [10, 11]. Nearly 40% of the world's gas reserves can be classified as being sour [11]. Currently, for conventional natural gas power plants, expensive and energy-intensive purification processes are done to remove H_2S and CO_2 before the methane is burned for power generation. At high concentrations of both, it is not practical or economical to extract the gas. As a result of this, a large fraction of world wide natural gas resources are currently unusable [10].

The objective of this work is to explore the use of sour gas directly as the fuel in an oxy-combustion power

plant for CCS. The utilization of this unusual fuel directly saves on the energy utilized for the purification process [9]. Furthermore, enhanced oil recovery (EOR) using CO_2 injection can increase the life of the reservoir by about 5-15% [12]. Currently in the literature, there is a lack of research on the utilization of sour gas as the fuel directly in power plants, and especially in oxy-combustion cycles. The issue of corrosion is the main hindrance to the progress and interest of using this gas directly. Once this knowledge gap has been addressed and tackled, these thermodynamic performance studies can then be used as inputs for future work focusing on the combustion behavior (ex. flame dynamics, reaction zone structures, stability) in these sour gas combustors, similar to what has been done for methane oxy-combustion [6, 13, 14].

Sour gas combustion produces SO_x and H_2SO_4 which can cause corrosion and also affect the transportation and storage of the CO_2 stream for EOR. Therefore an important part of the design is limiting the concentrations of these compounds in the products. Since sour gas technologies, specifically for oxy-combustion, has not received much attention, it is necessary to investigate different options for using this fuel to determine their viability and evaluate their potentials.

Oxy-fuel cycles have the great advantages of almost eliminating NO_x emissions, and also providing a simpler mechanism to capture CO_2 [14, 15]. The flame temperature in pure oxygen is very high and so a diluent is needed. The diluent used is usually some form of a recycled flue gases. For methane oxy-fuel cycles, several configurations have been studied in the literature. Semi-Closed Oxy-fuel Combustion Combined Cycles (SCOC-CC) [16, 17, 18, 19, 20] recycle part of the CO_2. In Water cycles [19, 21, 22, 23], H_2O is separated from the flue gases and recycled back to the combustor. The Graz cycle [16, 19, 24] adopts both CO_2 and H_2O recirculations.

The focus of this paper is on sour gas water cycles [21] with some modifications due to the presence of the sulfur compounds. As mentioned, this type of analysis is completely novel and has not been addressed in the literature before for sour gas. The water cycle can be categorized as a Rankine-type cycle with reheat and regeneration. Methane based water cycle working fluid consists mainly of H_2O and CO_2 (90/10 %vol.), whereas the sour gas case (as will be shown later), also has SO_x compounds in the working fluid which will affect the heat capacity of that stream and thus the power output in the turbines and also the performance of the whole cycle. These SO_x compounds affect the dew point temperature of the working fluid which can then cause acids to form and condense leading to corrosion issues in the low temperature components (ex. condenser, regenerator). Therefore, the sour gas cycles need to be modified.

There are four main areas and stages where the sulfur compounds pose problems in the cycle: fuel compression, expansion in the turbines, low temperature and condensation equipment, and in the CO_2 purification unit (CPU) for EOR. Since the fuel contains high levels of H_2S, corrosion is an extremely serious issue for the fuel compressors. Thomas et al. [25] suggested the use of the corrosion resistant alloy 20Cb-3 (Carpenter Alloy®), and the material's data sheet also recommends this alloy as having good corrosion

resistance to sour gas [26]. This material was used in the cost of electricity calculation as will be explained later on. After combustion, SO_x compounds are formed which can cause hot corrosion in the turbines (as will be explained in section 4.8), and the corrosive agent's deposition rate was found to be independent of the sulfur content [27]. Once again certain materials will have to be used which will further increase costs. The condensation of the working fluid, containing SO_x, leads to the formation of sulfuric acid which corrodes the components unless an acid-resistant material is used. The dew point temperature of the working fluid affects when this condensation occurs and so this is a critical design feature of these sour gas cycles. Finally, these sulfur compounds need to be removed from the system either through condensation and liquid separation or by a SO_x removal system (described in section 3.3.1). This is done in order to meet CO_2 transport and EOR constraints (ex. SO_2<100 ppm) and so these sulfur compounds need to be removed.

This paper is organized as follows: the methodology used in this analysis is briefly described in Section 2. In Section 3 the different sour gas water cycle configurations are described. In Section 4, the results of the analysis and cycle simulations are presented and discussed. Finally, Section 5 wraps up with the summary and conclusions of this work.

2. Methodology

Aspen Plus®[28] was used in the modeling analysis of the sour gas cycles. The PR-BM (Peng Robinson cubic equation of state with Boston-Mathias alpha function) property method [28] was used to model the combustors. When modeling other components, a different property method had to be used because of the unusual components in the working fluid: the sulfur compounds. The SR-Polar (Schwarzentruber and Renon equation-of-state model) property method was chosen to be the best fit for our application because it can be applied to highly polar components, e.g. SO_2 and SO_3, and recommended for high temperature and pressure applications.

Following an extensive literature review on methane oxy-fuel power cycles (since sour gas has never been addressed), two different configurations were considered for the sour gas water cycles: an acid resistance and a SO_x removal cycle. The Acid Resistance cycle is where we allow the working fluid, containing sulfur compounds, to condense. In this case, sulfuric acids form, which can corrode the components. Therefore, we assume that we use acid-resistant materials in order to protect the components where the acid is present. Acid resistant materials represent a major economic burden and can significantly increase costs, as will be shown later. The second type is the SO_x removal configuration, applied just before the working fluid condenses in the main cycle. All sulfur compounds are removed in this system and the exiting gas stream contains only mainly CO_2 with some Ar, N_2 (since the oxidizer is 95% O_2) and H_2O (similar to the pure methane cycles). This purified stream is used in the rest of the cycle. This configuration solves the problem of acid condensation, but as will be shown later there is an efficiency penalty associated with this SO_x

removal process.

These two cycles were simulated and a comparison was made with respect to the overall net efficiency, working fluid compositions and cost of electricity estimates. The modeling details and the results of this analysis are shown and discussed in the following sections.

3. Sour Gas Water Cycles

3.1. Modeling Assumptions

The important assumptions made when performing the thermodynamic modeling and simulations of the two sour gas water cycles are shown in Table 1. The same assumptions were applied to the Acid-Resistance and SO_x Removal cycles.

When modeling the combustor, the "RGibbs reactor" model was used [28]. RGibbs models single-phase chemical equilibrium, or simultaneous phase and chemical equilibria. The reaction kinetics are not taken into account. A Gibbs free energy minimization is done to determine the product composition. It is commonly used in the literature to model combustors when reactions occurring are not known, or are high in number due to the many components participating in the reactions. The combustion process was also assumed to be stoichiometric.

Because the combustors were modeled as equilibrium type combustors, this will grossly under-predict the SO_3 concentrations at the exit. Since the amount of SO_3 dictates how much acid forms in the latter stages of the cycle, it is important to try and improve the accuracy of the concentration of SO_3 in the working fluid. To do this, an additional reactor was added to model the SO_3 formation after the equilibrium combustor reactor (not shown in the cycle diagrams). The second reactor was modeled as an "RStoic" reactor in Aspen Plus [28]. This reactor was used only to model the formation of SO_3 from SO_2 using the single reaction: $SO_2 + \frac{1}{2}\,O_2 \longrightarrow SO_3$ with a specified conversion rate (SO_2/SO_3) of 1.5% obtained from [29]. The conditions that they tested were significantly different than ours (250-1000 ppm vs 11% SO_2), and so the conversion percentage chosen is really an upper limit and represents the most conservative estimate since the conversion ratio was found to decrease with increasing SO_2 concentration.

However in our cycle since the combustors are stoichiometric, there is not enough excess oxygen for the SO_2 to react with to achieve that conversion percentage. Thus the SO_3 concentration only increases by about 10-30 ppm (by volume) across that second reactor. In reality however, this SO_3 concentration actually decreases during expansion of the gas in the turbine [30] making our prediction even more conservative, since the mixture is essentially frozen during the expansions process. Also hot corrosion was found to be independent of the sulfur content in the working fluid [27] and so our SO_x concentrations estimations will not affect material selection.

	Sour Gas Water Cycles
Fuel	
Composition (mol%)	70% CH_4, 15% H_2S, 15% CO_2
Combustors	
Operating Pressures (bar)	100 & 15 (Main & Reheater)
Pressure Drops (%)	10 & 6 (Main & Reheater)
Turbines	
TIT's (°C)	600 & 1200 (HPT & LPT)
Isentropic Efficiencies (%)	87 & 90 (HPT & LPT)
Pumps	
Isentropic Efficiency (%)	75
Heat Exchangers	
Minimum Internal Temperature Approach (°C)	20
Pressure Drops (%)	5
ASU	
Specific Power (kWh/kg-O_2)	0.225
O_2 Stream Composition (mol%)	95% O_2, 4.2% Ar, 0.8% N_2
SO_x Removal System	
Gas Exit SO_2 Concentration	< 100 ppm
Liquid Exit pH	≈ 7
CPU	
CO_2 Delivery Pressure (bar)	110
Exit CO_2 Stream Composition (mol%)	$> 99\%$ CO_2 (EOR Ready)

Table 1: Sour gas water cycles modeling assumptions

For the low pressure turbine (LPT), we have chosen the reheater temperature to be 1200°C[1]. It was found that increasing the LPT inlet temperature had a bigger impact on efficiency than increasing the high pressure turbine (HPT) inlet temperature. A fixed combustor exit temperature of 600°C was chosen, and was controlled by the certain proportion of working fluid (water) that was recycled back to the combustor (stream 1 in Fig. 1). Turbine blade cooling for the LPT was not considered in this study. However, in reality, these high temperature turbines will definitely require cooling to be able to handle these temperatures. The abundance of water and cool steam (around 200°C) streams, could be used as the cooling fluids for these high temperature systems. But nonetheless, the main conclusions from this study are not expected to be significantly impacted.

The operating pressure of the combustor for the water cycle is 100 bar. Combustor pressure sensitivity did not impact the cycle efficiency or SO_x concentrations significantly enough to cause for changing this operating pressure away from what is commonly used in the literature [23, 32]. The reheater operates at 15 bar, which was found using a pressure sensitivity analysis (discussed later) to determine the optimum reheater pressure. The pressure drops for the two burners were taken as 10% and 6% for the combustor[2] and reheater respectively.

One key aspect of oxy-fuel combustion is the oxygen production process. Air separation units (ASU) using cryogenic separation is the only available option to produce the large amounts of oxygen required by these plants [34]. Cryogenic ASUs have significant energy penalties equivalent to 7-10% efficiency points.

The air separation unit model is similar to that of Hong et al. [35]. This ASU model produces an oxygen stream with an outlet oxygen purity (by volume) of 95% O_2, 4.2% Ar, 0.8% N_2 at a pressure of 1.24 bars, while requiring a specific power of 0.225 kWh/kg-O_2 (0.812 MJ/kg-O_2). This value is close to what is used in the literature [19].

The excess working fluid from the two cycles ('VAP' stream in Figures 1 and 5), is sent to a CO_2 purification unit (CPU) where the non-condensable gases (Ar & N_2) are removed and the capture-ready CO_2 stream is compressed up to 110 bar.

The incoming stream (mostly CO_2) to the CPU has the inert gases removed using low temperature separation techniques and the purified CO_2 stream is extracted as a liquid and pumped up to the sequestration pressure, and an exhaust stream consisting of mainly the inert gases is also produced. The separation process was modeled based on the layout of gas removal configuration B in [36]. This process was chosen because it delivers a liquid stream, thus eliminating the cost and energy penalty of gas phase compression of the purified stream. The separation technique also requires external refrigeration to provide the cooling load to

[1]As a reference, Clean Energy Systems (CES) has implemented an oxy-fuel water cycle for turbines with turbine inlet temperatures (TIT's) of 1080-1260°C [22, 31].

[2]As a reference, CES's gas generator is rated with a pressure drop of 10-15% [33]

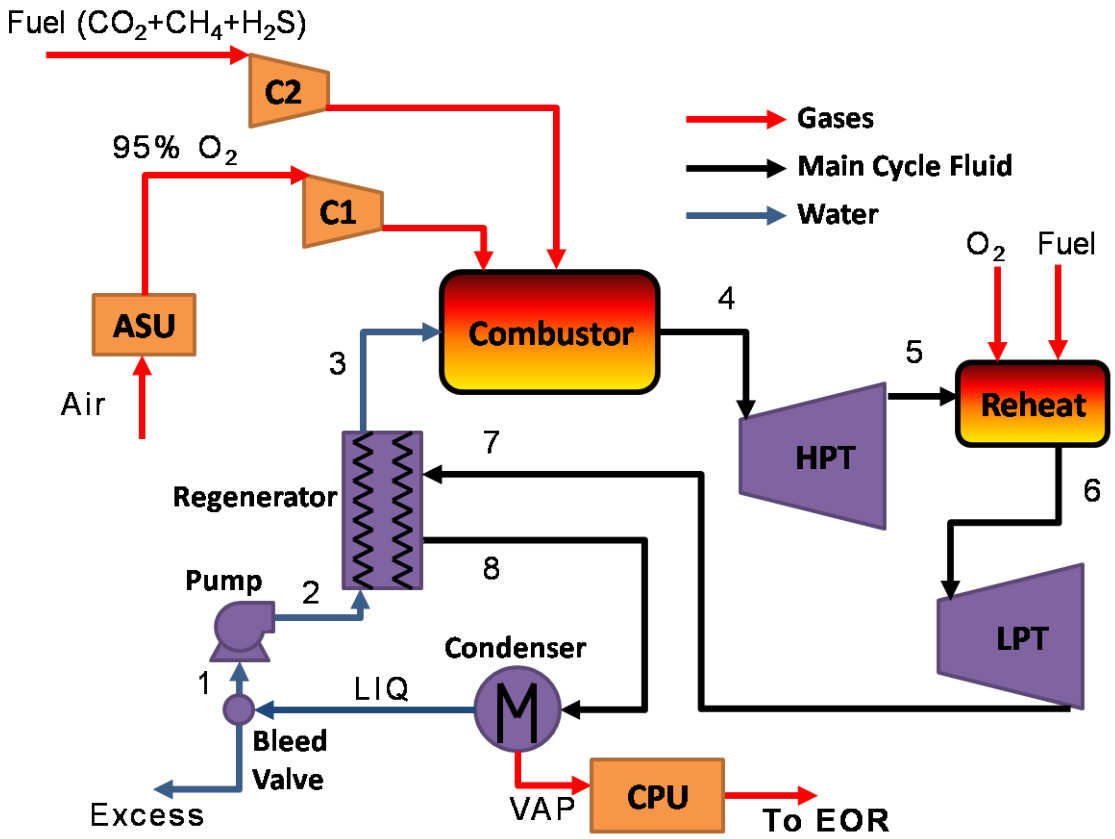

Figure 1: Overall process layout for the sour gas water cycle with acid resistance

the unit.

3.2. Acid Resistance Cycle

The "Acid Resistance Cycle" configuration is similar to the water cycle described in [19, 21, 22]. A similar component layout is adopted here with the difference being the fuel (70% CH_4, 15% H_2S, 15% CO_2) and the fact that acid resistant materials are used for all the cycle components where condensation occurs. Figure 1 shows the cycle diagram and components, with the corresponding T-s diagram in Figure 2. It is based on a Rankine cycle with reheat and regeneration.

Water at state 1 is pumped to 100 bar where it is preheated in the regenerator to about 247°C before entering the combustor. On the gas side, the oxygen stream from the air separation unit is sent to the combustor along with the fuel (70% CH_4, 15% H_2S, 15% CO_2), and the recycled working fluid (water). Water acts as a diluent in the combustor, and so the recycle ratio ($\dot{m}_1/\dot{m}_{LIQ}$) of the working fluid fixes the combustor exit temperature to 600°C. The main combustor flue gases (5% CO_2, 93% H_2O, 1% SO_2 by volume), state 4, are expanded in the high pressure turbine (HPT) to 15 bars to produce power. The

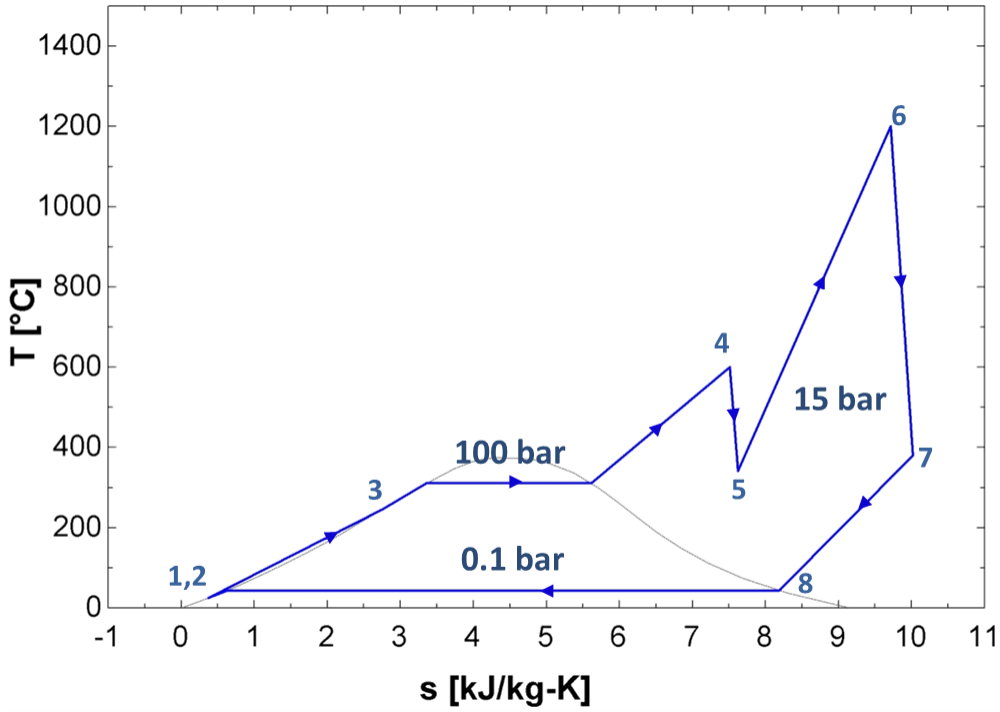

Figure 2: T-s diagram of the sour gas water cycle with acid resistance

working fluid at state 5 is reheated in the reheater where more fuel and oxygen are combusted to achieve a temperature of 1200°C. The reheater flue gases (10% CO_2, 88% H_2O, 2% SO_2, <1%Ar by volume), state 6, are expanded in the low pressure turbine (LPT) down to 0.1 bar.

Next, the hot working fluid enters the regenerator where it transfers its thermal energy to the water stream going to the combustor while being cooled down to state 8. The regenerator was divided up into two parts: a non-condensing heat exchanger and condensing heat exchanger. This was done to minimize the cost of acid resistance material needed in the regenerator; standard materials could be used for the non-condensing part and the expensive acid-resistant materials would only be required for the condensing section.

The remaining working fluid at state 8 is condensed to 25°C in the condenser and the vapor is separated out to be sent for EOR. Since the working fluid, containing sulfur compounds, is allowed to condense in the regenerator and condenser, sulfuric acid forms in those components, requiring acid resistant materials. After the condenser, 87% of the remaining liquid (water) is recycled back to the pump to be used as the dilution medium in the combustor. The vapor from the condenser is sent to the CPU and compressed to 110 bars. The CPU removes the inert compounds (Ar & N_2) but before this is done, the sulfur compounds are also removed. This SO_x removal system is described in detail in section 3.3.1. For these systems, no

extra water is needed to make up for the water that leaves with the vapor stream in the condenser and the 'Excess' stream in the bleed valve. At steady state, all the water formed in the combustor and reheater due to combustion, leave in the 'VAP' and 'Excess' streams.

The efficiency of this cycle with these conditions was found to be 40.9%. This is almost 0.5% points lower than the methane water cycle, which has the same layout and operating conditions but different fuel. The slight difference in efficiency can be attributed to the fact that the methane cycle has a working fluid with a slightly higher heat capacity (because of the higher CO_2 fraction) and as such produces more work in the turbines, increasing the efficiency.

A pressure sensitivity analysis was performed to investigate the effect of reheat pressure on the important cycle parameters. This analysis was performed on the sour gas and methane water cycles by varying the reheater pressure between 6-30 bars, and the results are shown in Figures 3 and 4. The reheater pressure was varied, instead of the combustor, because it was found to have a higher impact on cycle efficiency and SO_x concentrations. Because of the higher pressure ratio across the LPT and the higher TIT, a larger proportion of the power output came from the LPT.

Figure 3 shows the effect of varying pressure on the net cycle efficiencies. The efficiencies of both cycles increase with the pressure until a maximum is reached at about 15 bar. This is mainly because when the reheat pressure is changing, the fuel (and oxidizer) flow rates are continuously adjusted in order to maintain a 1200°C reheat exit temperature. This affects the total heat input to the cycle which in turn affects the efficiency. However, the pressure sensitivity analysis revealed that the efficiency did not vary by more than 0.5% when changing the pressure. The methane cycle also has about a 0.5% efficiency gain over the sour gas cycle, this is because the methane cycle's working fluid has a slightly larger heat capacity which produces more work and increases efficiency.

SO_2 and SO_3 concentrations (at the exit of the reheater) versus the pressure are shown in Figure 4. As can be seen, the reheater pressure had very little effect on both only causing a slight drop in the SO_3 fraction which are expressed in parts per million (ppm). This means that the system design in regards to acid formation and condensation will not be impacted, and if this cycle is implemented, changes in that reheater pressure during operation will not be a major concern.

3.3. SO_x Removal Cycle

This cycle was modeled in order to determine how the impact of removing the SO_x compounds from the working fluid affects the performance and cost. Figure 5 shows the cycle diagram and components, with the corresponding T-s diagram in Figure 6.

Water at state 1 is pumped to 100 bar, then preheated in the regenerator to about 260°C before entering the combustor. Oxygen from the ASU is sent to the combustor along with the fuel (70% CH_4, 15% H_2S, 15% CO_2), and the recycled working fluid (water). The recycle ratio ($\dot{m}_1/\dot{m}_{LIQ}$) fixes the combustor exit

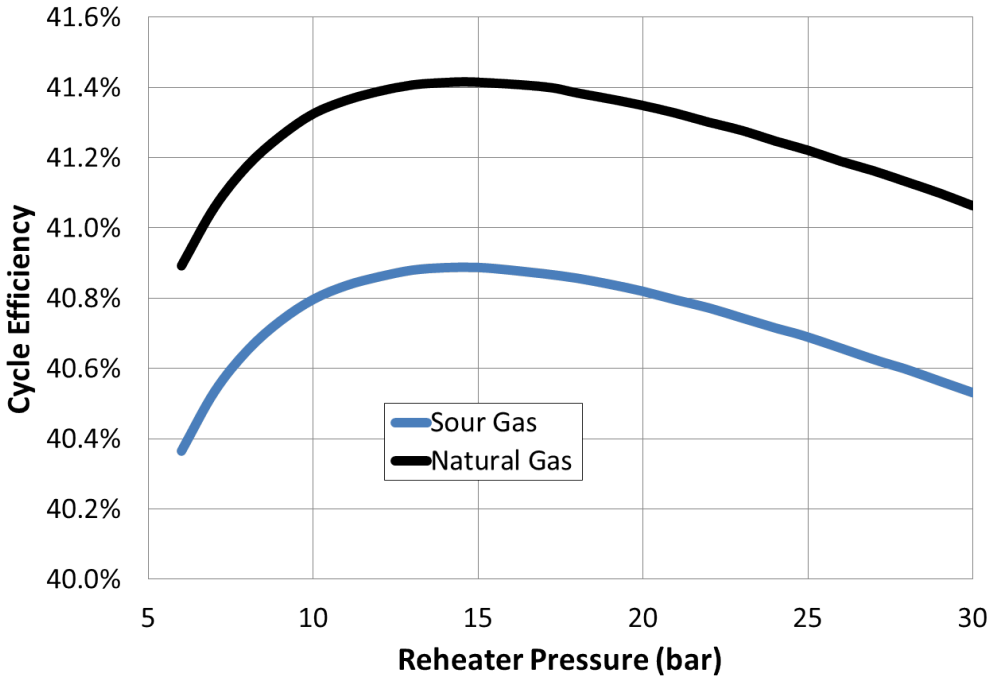

Figure 3: Effect of varying reheater pressure on the net cycle efficiency for the sour gas (acid resistance) and methane water cycles

temperature at 600°C. The combustor gases (5% CO_2, 93% H_2O, 1% SO_2 by volume), state 4, are expanded in the HPT to 15 bars. The fluid is then reheated where more fuel and oxygen are combusted to reach 1200°C. The exit stream (10% CO_2, 88% H_2O, 2% SO_2, <1%Ar by volume), state 6, are expanded in the low pressure turbine (LPT) down to 0.28 bar.

The low pressure fluid enters the regenerator where it transfers its thermal energy to the water stream going to the combustor while being cooled down to state 8. In this case, the working fluid is not allowed to condense in the regenerator by limiting the exit temperature to values higher than the dew point. The dew point of this cycle's working fluid (10% CO_2, 88% H_2O, 2% SO_2, <1%Ar by volume) was close to 203°C, and thus the hot stream exit temperature was fixed at 208°C while the cold stream's exit temperature was calculated such that the minimum internal temperature approach inside the heat exchanger was 20°C. At the exit of the regenerator the hot stream is sent to the SO_x removal system, leaving CO_2 with some Ar and N_2. The SO_x removal system is similar to the traditional flue gas desulfurization systems found in coal power plants where the flue gases are sprayed with a mixture of lime (CaO) and water which condenses and neutralizes the acidic mixture. SO_2 dissolves in the liquid and is separated from the gas stream. This process will be explained in greater detail later.

At the exit of the SO_x removal system, 82% of the liquid water is recycled back to the pump to act as

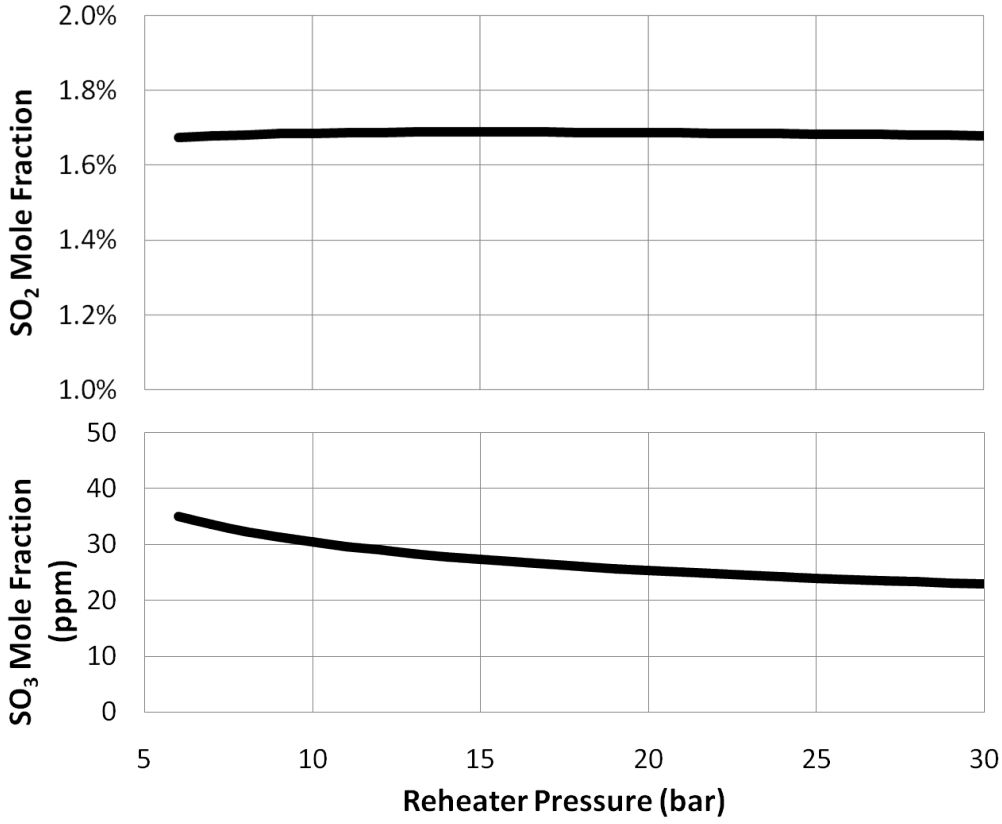

Figure 4: Effect of varying reheater pressure on the SO_2 and SO_3 concentrations at the exit of the reheater

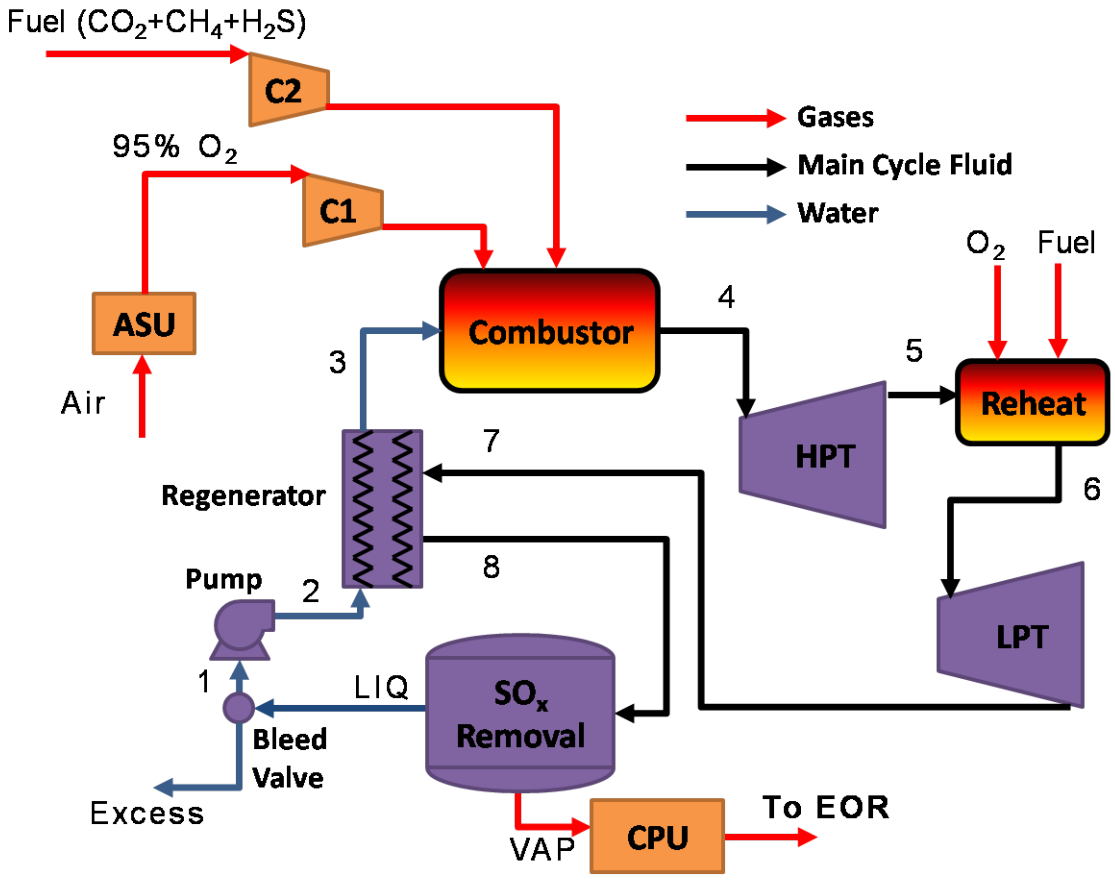

Figure 5: Overall process layout for the sour gas water cycle with SO_x removal

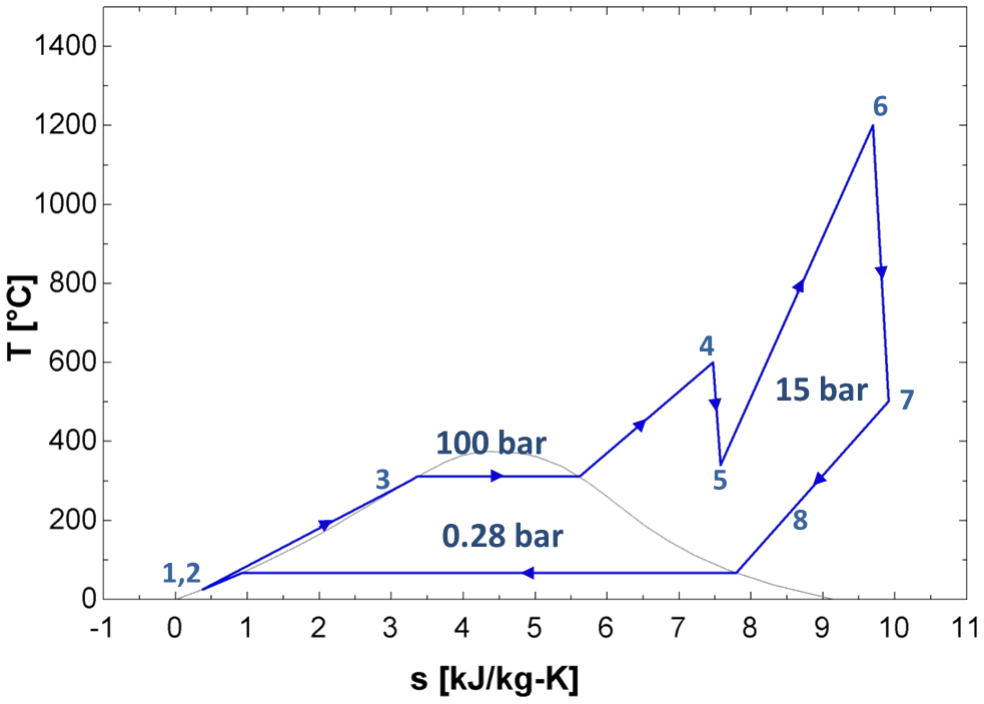

Figure 6: T-s diagram of the sour gas water cycle with SO_x removal

the dilution medium in the combustor. The vapor stream exiting the SO_x removal system, is sent to the CO_2 purification unit (CPU) and compressed up to 110 bars to a capture-ready carbon dioxide stream. The CPU removes the inert compounds from the working fluid (Ar & N_2).

The efficiency of this cycle was found to be 36.1%, about 4.5% points below the acid resistance cycle. Reasons include the slightly lower LPT pressure ratio and the energy requirement for the SO_x removal.

3.3.1. SO_x Removal System

The SO_x removal system modeled for the sour gas cycles, was based on the wet flue gas desulfurization (FGD) techniques [37]. The removal of these sulfur compounds prior to the working fluid condensing, allows us to limit the use of expensive acid resistant materials.

This system removes the S-compounds from the working fluid by reacting it with a lime solution (CaO + H_2O) and removing the byproducts as solid salts. The lime solution comes into direct contact with the working fluid and condenses the water and some SO_2 and SO_3. The SO_x compounds dissociate in the water to form ions and these react with the calcium ions present in the lime solution resulting in the formation of salts which eventually neutralize the effect of the acid. The salt formation creates a concentration gradient which drives more SO_2 and SO_3 to condense and dissolve in the water, thus prompting further flue gas desulfurization.

Figure 7 shows the system layout with all the components of the SO_x removal system. This system is similar to the direct contact condenser described by Zebian et al. [38]. The main goals of the design are to:

1. Keep the gas exit SO_2 concentration < 100 ppm (EOR constraints [39])
2. Keep the liquid exit pH $\simeq 7$

Before the CaO can react with the SO_2 and SO_3, both must be broken down into their respective ions. This is accomplished by dissolving the lime in water, which dissociates into Ca^{2+}, and spraying it into the flue gases to dissolve the SO_2. When the SO_2 condenses, it ionizes to form ${SO_3}^{2-}$. Similarly, when the SO_3 reacts with water it forms H_2SO_4 which then ionizes and forms ${SO_4}^{2-}$. These ions react with the Ca^{2+} and water to form salts. The corresponding reactions are shown below. These reactions, commonly used in FGD systems, were found to be mainly dependent on the amount of lime (CaO) input to the system. This amount is adjusted in order to achieve the two goals mentioned above. Reactions 9 and 10 are very important in the desulfurization process because the calcium salts are formed which are then removed as solids from the system, creating a gradient which furthers the dissolution of the calcium and sulfur compounds. The H_2SO_4 is formed through reaction 1 by reacting all of the SO_3 with the water in the working fluid. The water is an essential part of the FGD process and as such the appropriate amount was chosen to allow for all of these ionization reactions to take place. The system's operating pressure had a major impact on the efficiency and as such was chosen to maximize the cycle efficiency.

$$H_2O + SO_3 \longleftrightarrow H_2SO_4 \tag{1}$$

$$H_2O \longleftrightarrow OH^- + H^+ \tag{2}$$

$$H_2O + SO_2 \longleftrightarrow H^+ + HSO_3^- \tag{3}$$

$$HSO_3^- \longleftrightarrow H^+ + SO_3^{2-} \tag{4}$$

$$H_2SO_4 \longleftrightarrow H^+ + HSO_4^- \tag{5}$$

$$HSO_4^- \longleftrightarrow H^+ + SO_4^{2-} \tag{6}$$

$$CaO + H_2O \longrightarrow Ca(OH)^+ + OH^- \tag{7}$$

$$Ca(OH)^+ \longleftrightarrow Ca^{2+} + OH^- \tag{8}$$

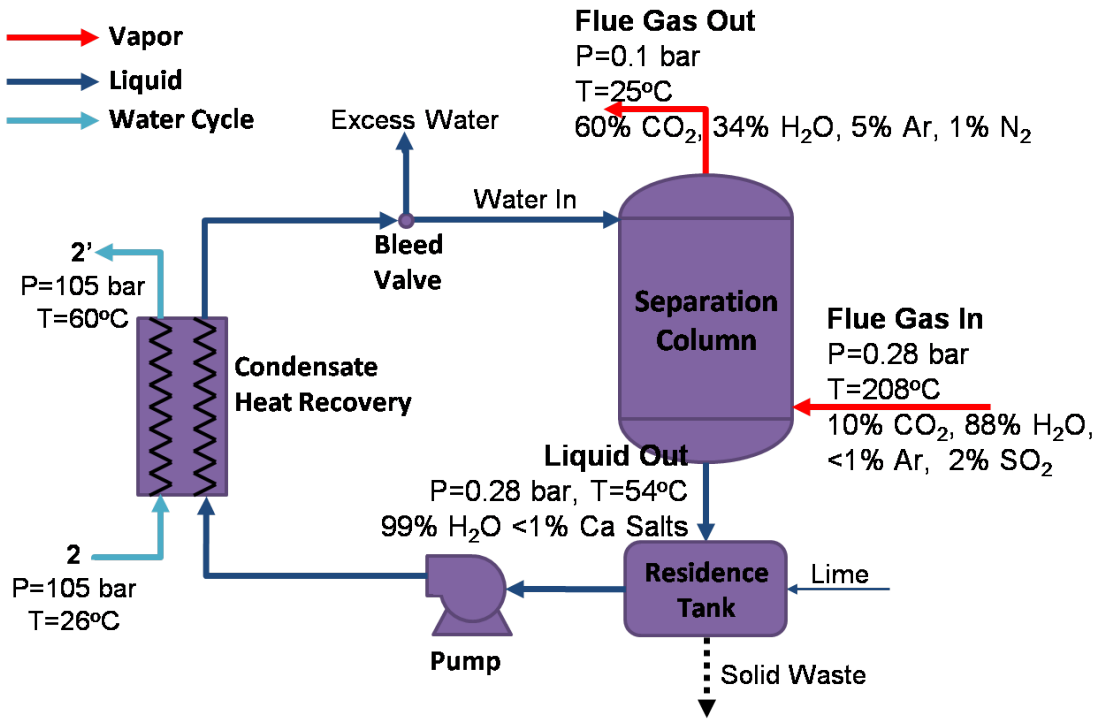

Figure 7: SO_x removal system implemented in the water cycle showing the operating conditions

$$Ca^{2+} + SO_4^{2-} + 2\,H_2O \longleftrightarrow CaSO_4 \cdot 2\,H_2O \tag{9}$$

$$Ca^{2+} + SO_3^{2-} + 2\,H^+ + 2\,OH^- \longleftrightarrow CaSO_3 + 2\,H_2O \tag{10}$$

The conditions and stream compositions for the system are also shown in Figure 7. The flue gas comes in directly from the exit of the regenerator, with a pressure that was chosen in order to maximize cycle efficiency and minimize pressure drop through the column. They exit the column at a temperature of around 49°C before being cooled further down to the condenser (not shown) temperature of 25°C. The gas flow rate coming in, for this case is 41 kg/s. On the other side, the water (+ lime) enters the column at the top with a mass flow rate of 625 kg/s after 4% of it was removed as excess in the bleed valve. The exiting liquid mixture at 54°C is sent to the residence tank where lime is added and the solids are removed. These reactions are exothermic and so the liquid temperature increases as it exits the tank. The amount of lime necessary for this cycle at these conditions was found to be 1.9 kg/s, this is the amount necessary for the "Liquid Out" stream to have neutral pH. The reagent stoichiometry, defined as $\frac{moles_{reagent}}{moles_{S-removed}}$, for the SO_x removal system was found to be 1.03 which is also exactly what traditional wet FGD systems operate at [40].

3.4. H_2O + CO_2 Recycle

In addition to the two sour gas water cycles, a cycle utilizing both H_2O and CO_2 recirculations was modeled to determine its performance when using sour gas as the fuel. This cycle has a similar layout to the Graz cycle [24], but with some modifications due to the new fuel composition and nature of the working fluid.

This cycle consists of a high temperature Brayton cycle and a low temperature Rankine cycle. In this case the main cycle working fluid exiting the compressor along with pure steam from the rankine cycle, is recycled to the combustor to act as the dilution medium. This results in a mixture of about 15% CO_2, 80% H_2O, 3% SO_2, 1% Ar by volume leaving the combustor at state 3. Since some CO_2 and SO_2 is also recycled, unlike the previous two cycles, this results in higher compositions of both of these in the main cycle fluid: 15% vs. 10% CO_2 and 3% vs. 2% SO_2.

The efficiency of this cycle with sour gas as the fuel, was calculated to be 24.8%, compared to a methane-based cycle which had an efficiency of 46.0%. This significant difference in efficiencies was due to the sulfur present in the working fluid which had a significant impact on the dew point of the sour gas cycle fluid. In the condenser, not all of the water is sent to the pump because depending on that recycle ratio, the composition of the working fluid of the cycle changes, and in turn affects the dew point of that stream. If that recycle ratio is too high then condensation occurs in the LPT which for this working fluid (containing H_2SO_4) would be severe. To prevent this condensation, a lower recycle ratio was chosen which resulted in a significant decrease in efficiency as was shown. Using this result, we concluded that this type of cycle with both H_2O and CO_2 recirculation is not a good option to use with sour gas as the fuel and as such this cycle was not discussed further.

4. Results and Discussion

4.1. T-s Diagrams

Comparing the T-s diagrams of the two sour gas water cycles, shown in Figures 2 and 6, the low pressure line is slightly higher for the SO_x Removal cycle than for the Acid Resistance cycle because of the higher pressure required for the SO_x removal system (0.3 vs 0.1 bar). As can be seen, the area inside the T-s diagram for the SO_x removal cycle is smaller and so we can estimate the efficiency to be lower, which is indeed the case. However, this may not always be the case since work is proportional to the area inside a T-s diagram only for ideal cycles.

4.2. Recycle Ratio

Figure 8 compares the recycle ratios for the systems. Since the Acid Resistance cycle has latent heat recovery in the regenerator, there is more energy available to transfer to the water stream being preheated. Thus the recycle ratio is higher for that cycle in order to recuperate that energy.

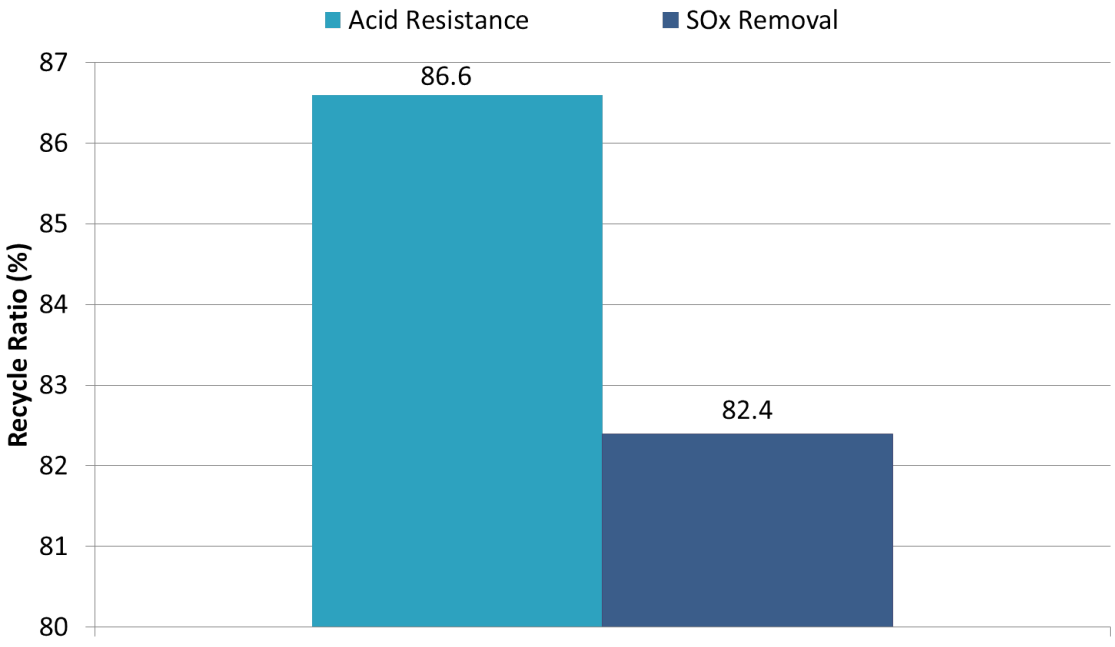

Figure 8: Recycle ratio comparison for the sour gas water cycles

4.3. Working Fluid

The working fluid of both cycles is the same at both the combustor and reheater exits. At the combustor exit, the composition is mainly: 5% CO_2, 93% H_2O, 1% SO_2, whereas at the reheater exit, it is mainly: 10% CO_2, 88% H_2O, 2% SO_2. Since the same working fluid is being recycled (liquid water) the exit of the combustor for both cycles also have the same compositions. At the reheater exit, the working fluids had higher SO_2 and CO_2 concentrations because the product gases from the combustion of fuel and oxygen are high in those two compounds. Therefore, when it mixes with the incoming working fluid, the total mole fraction of SO_2 and CO_2 goes up and H_2O goes down at the exit.

4.4. Sulfur Compounds Formation

The important sulfur compounds concentrations at every point in the cycle for the two sour gas water cycles are shown in Table 2. The state numbers shown refer to those in Figures 1 and 5. Firstly, it is evident that SO_2 is the major sulfur compound formed in these cycles with SO_3 and H_2SO_4 concentrations at ppm levels. All of the S-compounds fractions are about the same for both cycles at most points in the cycles, since the same type of diluent is recycled to the combustor. One important difference in the two cycles happens at states 7-8. For the acid resistance cycle, process 7-8 is the condensation step occurring in the regenerator which as can be seen, significantly increases the H_2SO_4 concentration in the working fluid by about 2 orders of magnitude due to the reaction of SO_3 with H_2O.

States	P (bar)		T (°C)		SO_2 (%)		SO_3 (ppm)		H_2SO_4 (ppm)	
	(a)	(b)	(a)	(b)	(a)	(b)	(a)	(b)	(a)	(b)
1	0.09	0.27	25	25	0	0	0	0	0	0
2	105.3	105.3	26.0	26.1	0	0	0	0	0	0
3	100	100	247.1	260.5	0	0	0	0	0	0
4	90	90	600	600	0.94%	0.92%	0.034	0.034	0.070	0.069
5	15	15	341.4	341.4	0.94%	0.92%	0.034	0.034	0.070	0.069
6	14.1	14.1	1200	1200	1.70%	1.68%	27	27	0.057	0.056
7	0.10	0.28	380.1	502.0	1.70%	1.68%	27	27	0.057	0.056
8	0.10	0.275	47	208	1.70%	1.68%	0	27	27.5	0.056

Table 2: Stream results and sulfur compounds compositions (mole fractions): (a) acid resistance cycle and (b) SO_x removal cycle

For the other cycle, however the H_2SO_4 concentration stays the same during process 7-8 since this cycle prevents the working fluid from condensing in order to limit the use of acid-resistant equipment. But after state 8, the stream is then sent to the SO_x removal system which is why the temperature and pressure of this stream are higher than those of the acid resistance cycle. This removes all of these sulfur compounds from that cycle's working fluid before then condensing the sulfur-free stream and then sending it to the CPU for inert gas removal. In the acid resistance cycle however, after state 8 the fluid is condensed even further and the gas then sent to the CPU where the S-compounds are removed. But at that point, the H_2SO_4 concentration increases even further due to the lower temperature and lower vapor quality. Finally it can also be seen that the SO_x fractions at the exit of the combustor (state 4) increase by about 1-2 orders of magnitudes after the reheat step (state 6) due to the combustion of more H_2S.

4.5. Pressure Drop Sensitivity

The following analysis presents the results from a combustor and reheater pressure drop sensitivity study that was done on the two cycles to determine their effect on the cycles' efficiencies. As can be seen from Figures 9 and 10, the combustor and reheater pressure drops were found not to have a significant effect on the efficiency.

The average slopes of the two graphs for the combustor analysis were determined to be the same at about -0.02 Eff%/Pdrop%. For the reheater analysis, the values were different with slopes of -0.03 and -0.04 Eff%/Pdrop% observed for the Acid Resistance and SO_x Removal cycles respectively. As can be seen, the reheater pressure drop had a slightly bigger impact on the efficiency for the two cycles. This is because the LPT contributes more to the net power output and so varying its inlet pressure (by changing the reheater

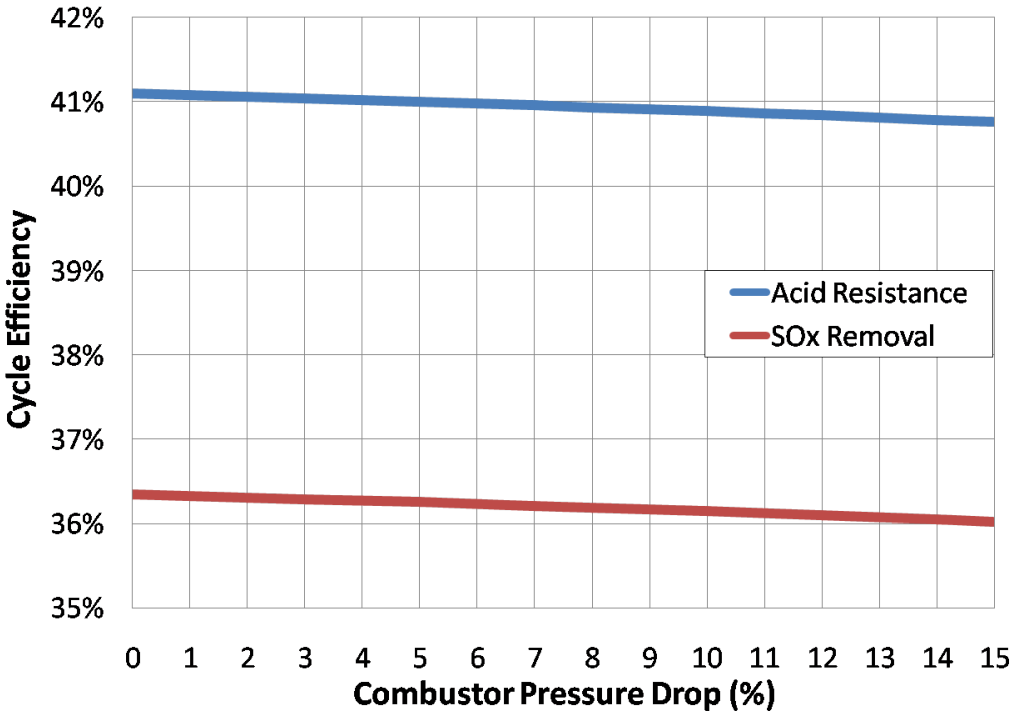

Figure 9: Effect of combustor pressure drop on net cycle efficiency for the sour gas water cycles

pressure drop), impacts the efficiency more significantly. In our analysis and for the results shown next, the default values of the pressure drops for the combustors and reheaters were taken to be 10% and 6% respectively.

4.6. Efficiency and Power Breakdown

The final and most important technical comparison of these cycles is shown in Figure 11. Details of the power generated and consumed by the different components in the cycles are shown where they are expressed as a function of the (total) heat input to the cycle (based on the fuel's LHV) in order to non-dimensionalize the results. The heat input to the two cycles were about 137 MW and 139 MW respectively. These values were calculated by Aspen Plus using a technical constraint in order to fix the exit temperature of the reheater.

The turbine work for the SO_x Removal cycle is lower than the Acid Resistance cycle because the low pressure is 0.3 compared to 0.1 bar. Therefore, there is a smaller pressure ratio across the turbine (LPT) and as a result less power is produced in the turbines. Due to the very low pressures that these turbines expand to, small changes in that outlet pressure can have a big impact on the power produced by the turbine. For these cycles, the density of the LPT outlet stream for the SO_x Removal cycle is about 2.4 times greater than that of the Acid Resistance cycle. This very large density difference at the turbine outlet results in a

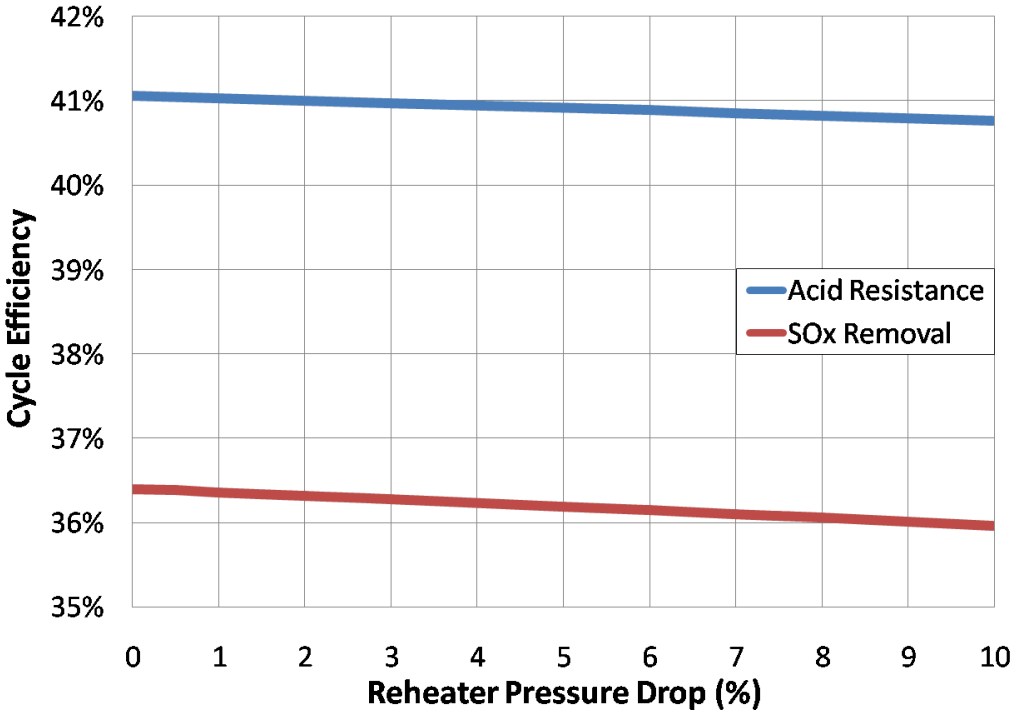

Figure 10: Effect of reheater pressure drop on net cycle efficiency for the sour gas water cycles

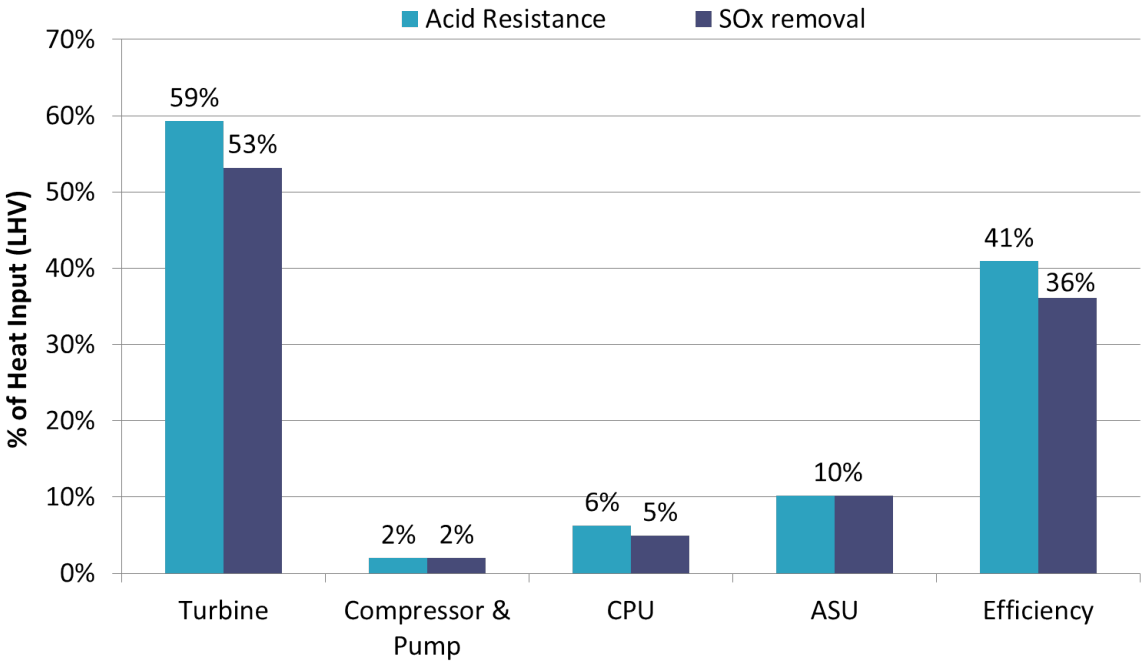

Figure 11: Power breakdown for the sour gas water cycles

large difference in the turbine works which results in the 6% efficiency reduction shown in the figure. The compressors and pump work for the two cycles are both very low, only resulting in a 2% efficiency loss.

The CPU (CO_2 Purification Unit) and ASU (Air Separation Unit) power inputs are fairly similar for both cycles. But a slightly smaller power is required in the CPU for the SO_x Removal cycle because the SO_x compounds are already being removed in the main cycle before entering the CPU. Therefore, there is no further efficiency penalty associated with this process, unlike the other cycle. The ASU is also the largest power consumer for both cycles as is common in oxy-combustion systems [7].

There is also an efficiency drop for the SO_x Removal cycle because of the inability to recuperate all of the latent energy from the hot working fluid in the regenerator. Since the hot working fluid doesn't condense for this cycle, less heat is transferred to the liquid water being preheated and so this overall leads to a smaller net power output and also lower efficiency.

4.7. Fuel Composition Sensitivity

4.7.1. H_2S Variations

Another important technical assessment of the sour gas cycle is the effect of fuel composition on the cycle performance. The most critical components in sour gas are H_2S and CO_2 since these two compositions vary widely depending on the lifetime and geography of the gas field. The acid resistance sour gas cycle performance was studied using the assumptions shown previously in Table 1 but with varying fuel compositions. Firstly, the results of H_2S variations in the fuel on the cycle are shown in Table 3. The cycle cost was found not to be sensitive to fuel composition changes and as such those results are not reported.

As the H_2S content in the fuel was increased, the recycle ratio also went up due to the change in heat capacity of the working fluid. As can be seen, the CO_2 and H_2O fractions decrease because the amount of methane in the fuel is decreasing which lowers the heat capacity as well. To compensate for that slight decrease in heat capacity, more of the diluent needs to be recycled to achieve the combustor and reheater exit temperatures. The amount of SO_2 in the working fluid increases due to the increase in H_2S content in the fuel. This increase in SO_2 in the working fluid did not have a significant impact on the efficiency as can be seen. The very slight increase is attributed to the fact that a smaller amount of CO_2 is now in the working fluid, as the H_2S increases, which slightly decreases the power requirement in the CPU. However the bigger impact from that increase in SO_2 content in the fluid, is in the SO_x removal system in the CPU where now more lime has to be used to remove more SO_2 from the working fluid.

4.7.2. CO_2 Variations

Next, variations in the CO_2 content in the fuel was studied and the results are shown in Table 4. Once again, the recycle ratio goes up with CO_2 content as the working fluid's heat capacity decreases due to the decrease in the H_2O fraction. Since the fuel's methane content is lower, the H_2O fraction in the working

Parameter		Cycle Results		
Fuel Composition (mol%)	CH_4	84	70	55
	H_2S	1	15	30
	CO_2	15	15	15
Recycle Ratio (%)		85.7	86.6	87.7
Working Fluid Composition (mol%)	CO_2	10.57	9.60	8.47
	H_2O	88.4	87.7	86.9
	SO_2	0.11	1.70	3.63
	Ar	0.80	0.81	0.83
	N_2	0.15	0.16	0.16
Net Efficiency (%)		40.8	40.9	41.1

Table 3: Fuel composition sensitivity results to H_2S variations

fluid also goes down even though the recycle ratio is increasing. However, the CO_2 and SO_2 fractions both increase with increasing CO_2 composition with the CO_2 fraction in the fluid reaching 16% at a CO_2 fuel composition of 50%. As in the previous fuel sensitivity, when the CO_2 content in the working fluid increases, the CPU power requirement goes up which, in this case, greatly affects the net cycle efficiency. The efficiency decreases by more than 3% as the CO_2 content in the fuel increases from 1 to 50%. Also the working fluid's heat capacity at lower CO_2 fuel concentrations is higher which increases the turbine power outputs and also further increasing the net efficiency.

4.8. Cost of Electricity

A preliminary cost analysis was also performed to estimate the capital cost of these cycles. Using this, the levelized cost of electricity (LCOE) was then calculated to bring in the impact of the cycle efficiency.

A critical part of the cost estimation procedure was the selection of the material for the different components. All of the sour gas cycles have SO_x in the working fluid and sulfuric acid forms where this working fluid condenses. Therefore, in order to protect the equipment from corrosion, certain material must be used. The selection was made based on literature recommendations. An important consideration is the problem of hot corrosion, defined as "the accelerated corrosion, resulting from the presence of salt contaminants, such as Na_2SO_4, that combined to form molten deposits, which damage the protective surface oxides" [41]. This Na_2SO_4 comes from the reaction of SO_2 in the working fluid with small concentrations of NaCl which is usually present in the combustion air if the plant is located near a sea, or from other industrial pollutants present in air. To combat this issue, it was found that increasing the chromium content in the metal alloys or coatings would significantly improve the resistance of the material. More specifically, nickel-based alloys

Parameter		Cycle Results		
Fuel Composition (mol%)	CH_4	84	70	35
	H_2S	15	15	15
	CO_2	1	15	50
Recycle Ratio (%)		85.7	86.6	92.3
Working Fluid Composition (mol%)	CO_2	8.27	9.60	16.30
	H_2O	89.30	87.70	79.88
	SO_2	1.46	1.70	2.88
	Ar	0.82	0.81	0.79
	N_2	0.16	0.16	0.15
Net Efficiency (%)		41.4	40.9	38.1

Table 4: Fuel composition sensitivity results to CO_2 variations

with chromium content greater than 15 wt.% were found to be more resistant to hot corrosion. The data also suggested that increasing titanium helps improve the material's hot corrosion resistance [42]. Based on these results, the best available material was chosen for the turbines and compressors that had SO_2 in the working fluid. This choice of material affects the equipment costs as will be seen later in Table 6.

Another important part of the material selection was that for the acid equipment. This refers to the components where the working fluid has condensed and sulfuric acid has formed. This is mainly for the condensing heat exchangers (condenser and regenerator) and the absorber column in the SO_x removal system. The model results presented show that the pH levels in these systems are expected to be very low thus making their environments very aggressive. To combat acid corrosion, a corrosion resistant material must be chosen that can withstand these extreme conditions. In a study by Shoemaker et al. [43] comparing the corrosion resistance of stainless steel metals, Alloy 686 (Iconel®) was found to be very stable in highly corrosive environments with sulfuric acid. As such, this material was chosen for the absorber shell cladding, and the shell and tube materials in the heat exchangers.

Using these material selections, the total equipment costs were calculated for the two cycles, and these were used as the Bare Erected Costs (BEC) when calculating the Levelized Cost of Electricity (LCOE). The Levelized Cost of Electricity (LCOE) calculation was performed based on the guidelines and assumptions discussed in the NETL report, Quality Guidelines for Energy System Studies: Cost Estimation Methodology for NETL Assessments of Power Plant Performance [44] and the assumptions that were used in this study are listed in Table 5. The results from this calculation are shown in Table 6 where the LCOE is shown for all of the cycles. The impact of the cycle efficiency plays a big role because the fuel cost is included in the LCOE calculations. We also considered what would happen in the limit that the fuel cost is very minimal

Parameter	Value
Engineering, Procurement and Construction Cost (EPCC)	
Engineering, Procurement and Construction (EPC) Contractor Services	9% of BEC
Total Plant Cost (TPC)	
Process Contingency	30% of EPCC
Project Contingency	25% of EPCC + Process Contingency
Total Overnight Cost (TOC)	
Owner's Costs	17.5% of TPC
Global Economic Assumptions	
Operational Period	25 years
Plant Capacity Factor	90%
Internal Rate of Return on Equity	10%
Income Tax Rate	38% Effective
Capital Depreciation	25 years, 200% declining balance
Variable O&M Costs Factor	1.5% of EPCC
Fixed O&M Costs Factor	3.5% of EPCC
Fuel Cost (only natural gas)	3 $/MMBTU [47]
Escalation of COE (revenue), O&M Costs, Fuel Costs (nominal annual rate)	3%

Table 5: LCOE economic modeling assumptions

and thus ≈ 0, and those results are also shown in the table.

Finally the costs of avoiding CO_2 emissions are shown in Table 6 for the two cycles and the two fuel cost scenarios. The cost of CO_2 avoided is calculated as the difference in the LCOE between the plant with CO_2 capture and that of a baseline plant without capture, divided by the difference in their CO_2 emissions in kg/MWh [45]. This value represents the average cost ($/ton) of reducing atmospheric CO_2 emissions by one ton while producing one MWh of electricity. The baseline plant chosen in this analysis is the gas-fired combined cycle without capture whose performance and costs were presented by Davison [46]. The choice of the reference plant for this calculation is very important as it can greatly impact the avoided cost and thus careful attention must be paid when comparing values from different technologies.

The two sour gas water cycles condense down to low pressures and so large heat exchangers are needed

for both which increases the equipment cost. Another issue with this low pressure is that in the CPU, more compression is needed to recompress the CO_2 for EOR which also results in further cost penalties. The SO_x removal cycle was found to have the overall lower cost than the acid resistance cycle. Costs savings are achieved from the fact that the expensive acid resistant materials don't need to be used for this cycle since the working fluid doesn't condense. Therefore, especially for the heat exchangers, the acid resistance cycle requires much more expensive equipment. As can be seen in the table, these choice of materials for the acid resistance cycle results in about a 20% increase in the equipment costs (BEC) over the SO_x removal case. It is known that errors and uncertainties in the cost estimation will inevitably be introduced depending on the method used or the source of the costs for components and materials. Thus we calculated the sensitivity of the LCOE to errors in the BEC. It was found that 10% variations in the BEC, resulted in an 8% change in the LCOE for both cycles. Similarly, 20% variations in the BEC caused the LCOE to change by 15% for the acid resistance cycle and 16% for the SO_x removal cycle.

Also as it turns out, although the acid resistance cycle has a higher efficiency than the SO_x removal one, its cycle cost is higher. Therefore a tradeoff would have to be made between cost and cycle performance. From a purely economic point of view, the LCOE result suggests that the SO_x Removal cycle is a better option than the Acid Resistance cycle. Since we don't have an exact number for the cost of the sour gas fuel, we also considered the case where the fuel cost is taken be 0. The LCOE results go down as expected and this helps give us a range of what one might expect depending on what the fuel cost is. Worst case, the LCOE for the SO_x removal cycle would be around 126 \$/MWh and in the best case scenario this cost goes down to 101 \$/MWh, a 20% decrease. The LCOE of a methane oxy-fuel cycle was found to be around 117 (2014 \$/MWh) [46]. Since the majority of the methane oxy-fuel cycle modeling in the literature don't include the energy and cost penalties of the natural gas processing step, it is hard to make an accurate recommendation on which sour gas treatment option is more feasible: pre-combustion gas sweetening vs burning gas directly. However as can be seen, when the fuel is assumed to be very cheap (cost $\approx$ 0) the LCOE of the sour gas cycles are actually both cheaper than the methane oxy-fuel cycle.

The cost of CO_2 avoided for the two cycles is calculated to be 184 \$/ton and 151 \$/ton for the acid resistance and SO_x removal cycles respectively. Just as a reference, Davison [46] found the CO_2 avoided cost for a natural gas oxy-fuel cycle to be 120 \$/ton (after conversion to 2014 \$). Therefore the cost of reducing CO_2 emissions while supplying the same amount of electricity for the two sour gas cycles, only becomes competitive and even cheaper than the natural gas cycle when the sour gas fuel cost is considered negligible, as shown in Table 6. However due to the uncertainties and assumptions that go into the CO_2 avoided cost calculation (ex. choice of reference plant), arguably the measure that is most relevant for technical, economic and policy analyses, is the levelized cost of electricity.

Parameter	Unit	Acid Resistance	SO_x Removal
Net Power Output	MW	55.98	50.04
Net Efficiency	%	40.9	36.1
BEC	MM$	131	103
EPCC	MM$	143	112
TOC	MM$	260	203
LCOE	2014 $/MWh	**138**	**126**
LCOE (Fuel Cost = 0)	2014 $/MWh	**116**	**101**
Cost of CO_2 Avoided	$/ton	184	151
Cost of CO_2 Avoided (Fuel Cost = 0)	$/ton	121	80

Table 6: Costing analysis results for the sour gas water cycles

5. Conclusions

Methane oxy-fuel water cycles have been extensively studied in the literature, whereas sour gas cycles have received no attention thus far. A detailed analysis of oxy-fuel water cycles fueled by sour gas has been performed in this study. The water cycles were subdivided into two configurations for addressing issues and limitations associated with the presence of sulfur compounds in the fuel.

An Acid Resistance and a SO_x Removal cycle were considered. It was found that the Acid Resistance cycle had the better efficiency of 40.9%, the main reason being the fact that the working fluid is allowed to condense in the regenerator and so some of its latent heat is recuperated. Changes in the CO_2 composition in the fuel was found to have a bigger impact on system performance than H_2S variations as it significantly affected the CPU power requirement and thus the efficiency.

A preliminary cost analysis was also done and the levelized cost of electricity was calculated to bring in the impact of cycle efficiency. It was found that the SO_x Removal cycle to be cheaper, as we had predicted, since the working fluid doesn't condense in the cycle and so less amounts of expensive acid resistant equipment need to be used. The LCOE of the SO_x Removal cycle was found to be 126 $/MWh compared to 138 $/MWh for the Acid Resistance cycle.

Since the fuel is cheap, sacrificing some efficiency points at the expense of a less costly system would not be a major issue. Therefore from this whole analysis it seems that the best process cycle to use is the SO_x Removal water cycle.

In future work, a similar analysis will be done that focuses on another type of cycle configuration namely, the sour gas combined cycles.

6. Acknowledgments

The authors would like to thank Siemens for sponsoring this work. Aspen Plus® was generously provided by Aspen Technology.

References

[1] United States Environmental Protection Agency (EPA), Global Greenhouse Gas Emissions Data, http://www.epa.gov/climatechange/ghgemissions/global.html (2013).

[2] Energy Information Administration, International Energy Outlook, report DOE/EIA-0484 (2013).

[3] D. Gielen, The future role of CO_2 capture and storage: results of the IEA-ETP Model, report no. EET/2003/04, http://www.iea.org/textbase/papers/2003/eet04.pdf (2003).

[4] V. Tola, A. Pettinau, Power generation plants with carbon capture and storage: A techno-economic comparison between coal combustion and gasification technologies, Applied Energy 113 (0) (2014) 1461 – 1474. doi:http://dx.doi.org/10.1016/j.apenergy.2013.09.007.
URL http://www.sciencedirect.com/science/article/pii/S0306261913007538

[5] A. Pettinau, F. Ferrara, C. Amorino, Techno-economic comparison between different technologies for a {CCS} power generation plant integrated with a sub-bituminous coal mine in italy, Applied Energy 99 (0) (2012) 32 – 39. doi:http://dx.doi.org/10.1016/j.apenergy.2012.05.008.
URL http://www.sciencedirect.com/science/article/pii/S030626191200356X

[6] M. A. Nemitallah, M. A. Habib, Experimental and numerical investigations of an atmospheric diffusion oxy-combustion flame in a gas turbine model combustor, Applied Energy 111 (0) (2013) 401 – 415. doi:http://dx.doi.org/10.1016/j.apenergy.2013.05.027.
URL http://www.sciencedirect.com/science/article/pii/S0306261913004285

[7] B. Metz, O. Davidson, H. De Coninck, M. Loos, L. Meyer, IPCC, 2005: IPCC special report on carbon dioxide capture and storage. Prepared by Working Group III of the Intergovernmental Panel on Climate Change, Cambridge, United Kingdom and New York, NY, USA, 442 pp.

[8] US Energy Information Administration, Average national levelized costs for generating technologies in 2018 (2011).

[9] F. Garca-Labiano, L. de Diego, P. Gayn, A. Abad, A. Cabello, J. Adnez, G. Sprachmann, Energy exploitation of acid gas with high {H2S} content by means of a chemical looping combustion system, Applied Energy 136 (0) (2014) 242 – 249. doi:http://dx.doi.org/10.1016/j.apenergy.2014.09.

041.
URL http://www.sciencedirect.com/science/article/pii/S0306261914009891

[10] W. Burgers, P. Northrop, H. Kheshgi, J. Valencia, Worldwide development potential for sour gas, Energy Procedia 4 (0) (2011) 2178 – 2184, 10th International Conference on Greenhouse Gas Control Technologies. doi:http://dx.doi.org/10.1016/j.egypro.2011.02.104.
URL http://www.sciencedirect.com/science/article/pii/S1876610211003018

[11] Total, France, Sour gas: A history of expertise (2007).

[12] ICO2N, Enhanced Oil Recovery - a significant economic opportunity to help jump-start Carbon Capture and Storage, http://www.ico2n.com/wp-content/uploads/2011/08/ICO2N-EOR-Fact-Sheet.pdf (2011).

[13] A. P. Shroll, S. J. Shanbhogue, A. F. Ghoniem, Dynamic-stability characteristics of premixed methane oxy-combustion, Journal of Engineering for Gas Turbines and Power 134 (5) (2012) 051504.

[14] C. Liu, G. Chen, N. Sipcz, M. Assadi, X. Bai, Characteristics of oxy-fuel combustion in gas turbines, Applied Energy 89 (1) (2012) 387 – 394, special issue on Thermal Energy Management in the Process Industries. doi:http://dx.doi.org/10.1016/j.apenergy.2011.08.004.
URL http://www.sciencedirect.com/science/article/pii/S0306261911004995

[15] J. D. Figueroa, T. Fout, S. Plasynski, H. McIlvried, R. D. Srivastava, Advances in {CO2} capture technologythe u.s. department of energy's carbon sequestration program, International Journal of Greenhouse Gas Control 2 (1) (2008) 9 – 20. doi:http://dx.doi.org/10.1016/S1750-5836(07)00094-1.
URL http://www.sciencedirect.com/science/article/pii/S1750583607000941

[16] W. Sanz, H. Jericha, B. Bauer, E. GÃķttlich, Qualitative and quantitative comparison of two promising oxy-fuel power cycles for CO_2 capture, Journal of Engineering for Gas Turbines and Power 130 (3) (2008) 031702.

[17] G. Corchero, V. Timon, J. Montanes, A natural gas oxy-fuel semiclosed combined cycle for zero CO_2 emissions: a thermodynamic optimization, Proceedings of the Institution of Mechanical Engineers, Part A: Journal of Power and Energy 225 (4) (2011) 377–388.

[18] O. Bolland, P. Mathieu, Comparison of two CO_2 removal options in combined cycle power plants, Energy Conversion and Management 39 (1618) (1998) 1653 – 1663. doi:http://dx.doi.org/10.1016/S0196-8904(98)00078-8.
URL http://www.sciencedirect.com/science/article/pii/S0196890498000788

[19] H. M. Kvamsdal, K. Jordal, O. Bolland, A quantitative comparison of gas turbine cycles with capture, Energy 32 (1) (2007) 10 – 24. doi:http://dx.doi.org/10.1016/j.energy.2006.02.006.
URL http://www.sciencedirect.com/science/article/pii/S036054420600048X

[20] F. Franco, T. Mina, G. Woolatt, M. Rost, O. Bolland, Characteristics of cycle components for CO_2 capture, in: Proceedings of 8th International Conference on Greenhouse Gas Control Technologies, Trondheim, Norway, 2006.

[21] R. Anderson, H. Brandt, H. Mueggenburg, A power plant concept which minimizes the cost of carbon dioxide sequestration and eliminates the emission of atmospheric pollutants, Greenhouse Gas Control Technologies (1999) 59.

[22] R. E. Anderson, S. MacAdam, F. Viteri, D. O. Davies, J. P. Downs, A. Paliszewski, Adapting gas turbines to zero emission oxy-fuel power plants, in: ASME Turbo Expo 2008: Power for Land, Sea, and Air, American Society of Mechanical Engineers, 2008, pp. 781–791.

[23] C. Gou, R. Cai, H. Hong, An advanced oxy-fuel power cycle with high efficiency, Proceedings of the Institution of Mechanical Engineers, Part A: Journal of Power and Energy 220 (4) (2006) 315–325.

[24] W. Sanz, H. Jericha, F. Luckel, F. Heitmeir, A further step towards a Graz cycle power plant for CO_2 capture, ASME Paper GT2005-68456, ASME Turbo Expo.

[25] D. Thomas, S. Benson, Carbon Dioxide Capture for Storage in Deep Geologic Formations-Results from the CO2 Capture Project: Vol 1-Capture and Separation of Carbon Dioxide from Combustion, Vol 2-Geologic Storage of Carbon Dioxide with Monitoring and Verification, Elsevier, 2005.

[26] Carpenter, 20Cb-3 Stainless Technical Data Sheet (2011).

[27] M. Steinberg, K. Schofield, The controlling chemistry of surface deposition from sodium and potassium seeded flames free of sulfur or chlorine impurities, Combustion and Flame 129 (4) (2002) 453 – 470. doi:http://dx.doi.org/10.1016/S0010-2180(02)00363-2.
URL http://www.sciencedirect.com/science/article/pii/S0010218002003632

[28] Aspen Technologies Inc, Aspen Plus (2012).

[29] D. Fleig, M. U. Alzueta, F. Normann, M. Abin, K. Andersson, F. Johnsson, Measurement and modeling of sulfur trioxide formation in a flow reactor under post-flame conditions, Combustion and Flame 160 (6) (2013) 1142 – 1151. doi:http://dx.doi.org/10.1016/j.combustflame.2013.02.002.
URL http://www.sciencedirect.com/science/article/pii/S0010218013000448

[30] D. Bongartz, A. F. Ghoniem, Chemical kinetics mechanism for oxy-fuel combustion of mixtures of hydrogen sulfide and methane, Combustion and Flame (0) (2014) –. doi:http://dx.doi.org/10.1016/j.combustflame.2014.08.019.
URL http://www.sciencedirect.com/science/article/pii/S0010218014002661

[31] R. Anderson, F. Viteri, R. Hollis, A. Keating, J. Shipper, G. Merrill, C. Schillig, S. Shinde, J. Downs, D. Davies, et al., Oxy-fuel gas turbine, gas generator and reheat combustor technology development and demonstration, in: ASME Turbo Expo 2010: Power for Land, Sea, and Air, American Society of Mechanical Engineers, 2010, pp. 733–743.

[32] S. H. Tak, S. K. Park, T. S. Kim, J. L. Sohn, Y. D. Lee, Performance analyses of oxy-fuel power generation systems including CO_2 capture: comparison of two cycles using different recirculation fluids, Journal of mechanical science and technology 24 (9) (2010) 1947–1954.

[33] Clean Energy Systems, http://www.cleanenergysystems.com, accessed: 02-24-2014.

[34] C. Fu, T. Gundersen, Using exergy analysis to reduce power consumption in air separation units for oxy-combustion processes, Energy 44 (1) (2012) 60–68.

[35] J. Hong, G. Chaudhry, J. Brisson, R. Field, M. Gazzino, A. F. Ghoniem, Analysis of oxy-fuel combustion power cycle utilizing a pressurized coal combustor, Energy 34 (9) (2009) 1332–1340.

[36] C. O. Iloeje, Process modeling and analysis of CO_2 purification for oxy-coal combustion, Master's thesis, Massachusetts Institute of Technology, Cambridge, MA, USA (2011).

[37] R. K. Srivastava, W. Jozewicz, Flue gas desulfurization: The state of the art, Journal of the Air & Waste Management Association 51 (12) (2001) 1676–1688.

[38] H. Zebian, N. Rossi, M. Gazzino, D. Cumbo, A. Mitsos, Optimal design and operation of pressurized oxy-coal combustion with a direct contact separation column, Energy 49 (2013) 268–278.

[39] U.S. Department of Energy - National Energy Technology Laboratory, Advanced oxy-combustion technology development and scale-up for new and existing coal-fired power plants (DE-FOA-0000636).

[40] R. Gaikwad, W. Boward, W. DePriest, Wet flue gas desulfurization technology evaluation, Sargent and Lundy, LLC, prepared for National Lime Association, project (11311-000).

[41] N. Eliaz, G. Shemesh, R. Latanision, Hot corrosion in gas turbine components, Engineering failure analysis 9 (1) (2002) 31–43.

[42] G. Y. Lai, High-temperature corrosion and materials applications, ASM International, 2007.

[43] L. Shoemaker, J. R. Crum, Experience in effective application of metallic materials for construction of fgd systems (2010).

[44] National Energy Technology Laboratory, Quality guidelines for energy system studies: cost estimation methodology for NETL assessments of power plant performance, U.S. Department of Energy (2011).

[45] M. R. Abu-Zahra, J. P. Niederer, P. H. Feron, G. F. Versteeg, {CO2} capture from power plants: Part ii. a parametric study of the economical performance based on mono-ethanolamine, International Journal of Greenhouse Gas Control 1 (2) (2007) 135 – 142, 8th International Conference on Greenhouse Gas Control Technologies GHGT-8. doi:http://dx.doi.org/10.1016/S1750-5836(07)00032-1.
URL http://www.sciencedirect.com/science/article/pii/S1750583607000321

[46] J. Davison, Performance and costs of power plants with capture and storage of {CO2}, Energy 32 (7) (2007) 1163 – 1176. doi:http://dx.doi.org/10.1016/j.energy.2006.07.039.
URL http://www.sciencedirect.com/science/article/pii/S0360544206002155

[47] US Energy Information Administration, Natural Gas, http://www.eia.gov/naturalgas/weekly/ (2014).